UCRL-JC-119326
PREPRINT
CONF-950793--44

X-Ray Cameras for >5 keV Imaging

O. L. Landen
P. M. Bell
D. H. Kalantar
D. K. Bradley

This paper was prepared for submittal to
SPIE 1995 International Symposium on Optical Science, Engineering and Instrumentation
San Diego, CA
July 9-14, 1995

July 20, 1995

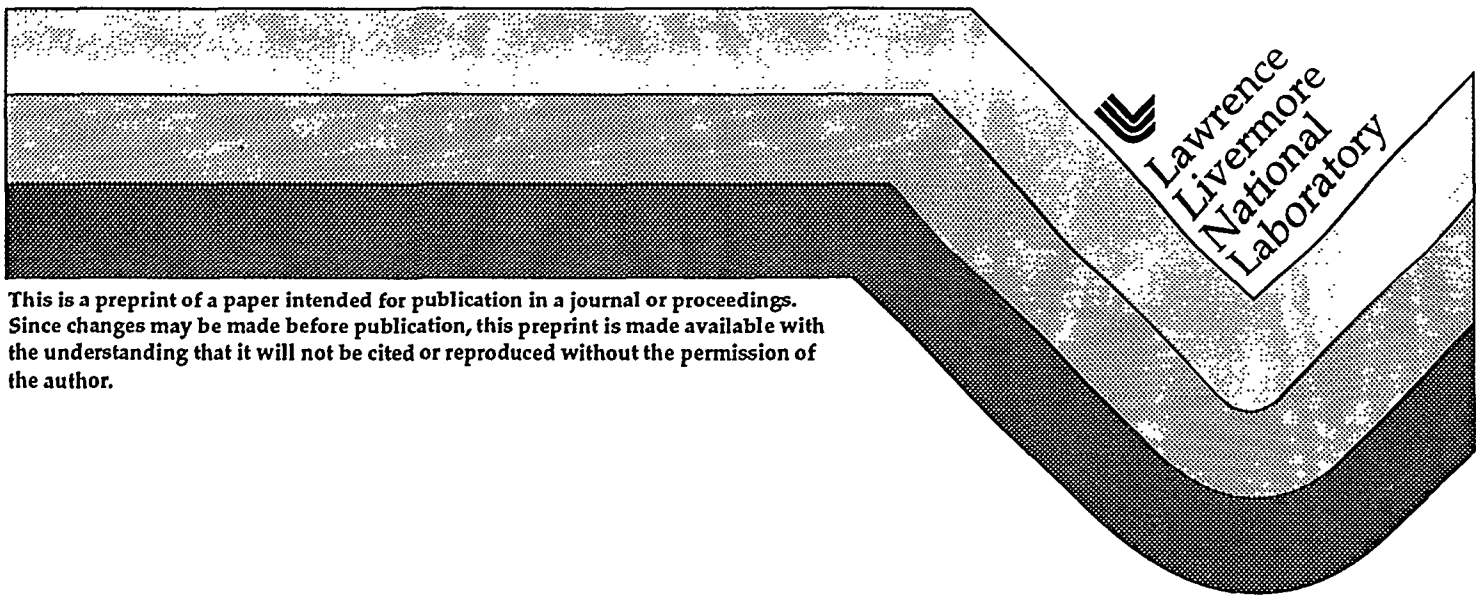

X-ray Framing Cameras for > 5 keV Imaging

O.L. Landen, P.M. Bell, R. Costa, D.H. Kalantar, and D.K. Bradley*

Lawrence Livermore National Laboratory, P.O. Box 5508, Livermore, CA 94550
*Laboratory for Laser Energetics, University of Rochester, 250 E. River Road, Rochester, NY 14623

ABSTRACT

Recent and proposed improvements in spatial resolution, temporal resolution, contrast, and detection efficiency for x-ray framing cameras are discussed in light of present and future laser-plasma diagnostic needs. In particular, improvements in image contrast above hard x-ray background levels is demonstrated by using high aspect ratio tapered pinholes.

Keywords: microchannel-plate, x-ray framing camera

1. INTRODUCTION

Gated, microchannel-plate-based (MCP) framing cameras[1-4] have been deployed worldwide for 0.2 - 7 keV x-ray imaging of 0.1 - 10 ns duration laser-plasma phenomena. The progression to larger lasers and targets and higher plasma temperatures in inertial confinement fusion (ICF) research will make time-resolved imaging at the higher photon energies even more viable, more relevant and sometimes imperative in cases where optically-thin imaging must be preserved. In addition, research in hot electron production and energy deposition mechanisms during short ultra-high-power laser-plasma interactions should benefit from ≥ 10 keV gated imaging capabilities. In the area of characterization, coated and uncoated MCP sensitivities below ≈ 5 keV have been extensively measured under dc conditions[5,6]. However, there are new issues associated with gated MCP framing camera operation above 5 keV. The degradation in spatial resolution and contrast from using two rather than one MCP to enhance gain for ultrashort gated operation (< 40 ps) has suggested thinner single-plates are the best course to shorter gate durations. The various factors degrading present signal-to-noise have been quantified. The spatial and temporal properties of gated MCPs can be also modified (degraded) by the longer mean free paths of hard x-rays leading to a distributed photocathode. As a means of improving ultrahard x-ray rejection, an adaptation of an x-ray collimator[7] is presented as the basis for future high-aspect-ratio (> 100) pinhole imaging.

2. HARD X-RAY GATED DETECTION

2.1 Spatial and temporal resolution

The first generation Nova Facility framing cameras[8] used 10 μm diameter pore, 400 μm thick (L/D = 40) plates yielding minimum gate widths of ≈ 80 ps. The subsequent quest for higher gating speeds in MCP-based framing cameras has followed two approaches[9,10]. The first design consists of using a thinner, 5 μm pore L/D = 40 plate which halves electron transit times allowing for shorter (≈ 40 ps) gate pulses (denoted FFC 2). The second design consisted of two MCPs of 10 μm pore diameter placed back-to-back (denoted FFC 1). The first thinner MCP has an L/D = 20 which provides low gain gating with again reduced electron transit times. The second L/D = 40 plate is run dc and provides the necessary additional gain. This camera suffered from reduced contrast due to a penetrating hard x-ray component ejecting photoelectrons at the second plate. Moreover, the combination of two plates was expected to have a wider line-spread function than exhibited by the usual single-plate framing camera. To measure the spatial resolution, a 10-μm-wide, 1-mm-long slit placed near the MCP was backlit by 1.5, 3, 4.5 and 7.5 keV dc X-ray sources. The measured line-spread functions, digitized at 5 by 5 μm pixel size and averaged over the central 95% of the slit length, are shown on Fig. 1. The two-plate camera exhibits a 56 μm FWHM versus a 27± 3 μm FWHM for the usual 10 μm pore single-plate design at all photon energies up to 7.5 keV. The 6 μm pore FFC 2 MCP shows similar spatial resolution as the thicker single-plate, principally limited by the finite gap between MCP and phosphor electron-to-light conversion layer[11,12]. Since both cameras produce similar 30 - 40 ps gate widths for similar gain, the single-plate design is now favored. Hence, further improvements in gate speed are

expected to follow the path of thinner plates and smaller pore size. As discussed further, there are other benefits to reducing MCP volume.

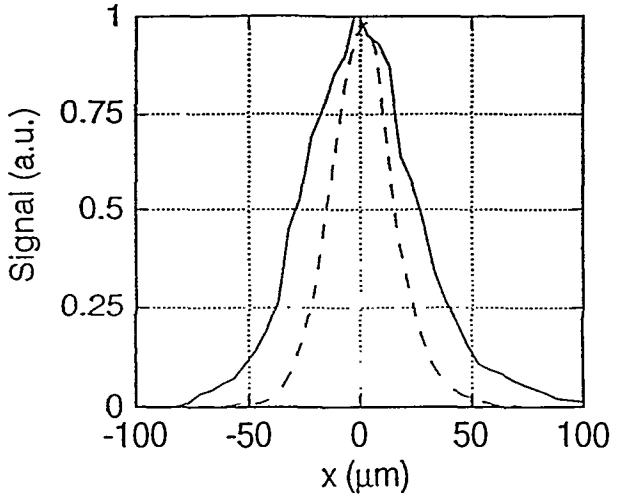

Figure 1 Measured line spread function for single-plate (dashed curve) and double-plate (solid curve) MCP camera.

It is well known that even for MCPs coated with an efficient photocathode material at the top surface (e.g. Au or CsI), photoelectrons are also produced in the uncoated leaded glass[13]. Above 10 keV, photons will easily[9] traverse several 1 μm pore walls at a typical bias angle of 8°, hence increasing the relative photoelectric contribution from the uncoated sections of the MCP. This distributed photocathode will in turn degrade spatial resolution and, secondly, modify the simple estimates of gate profiles[14,15] based on photoelectrons born only at the front surface. The degradation in spatial resolution can be minimized by again using thinner plates and minimizing the pore bias angle. For example, 6° over L = 200 μm yields ≈ 20 μm resolution, a worst case estimate since there is gain along the length of the pores. Third, spectral and angular sensitivities will differ between dc and gated operation as the relative gains between photoelectrons born deep in the MCP pores and at the front Au coating will depend on the gate voltage profile. The latter two issues become increasingly important for the standard operating conditions in which the shutter speed is minimized by setting the voltage profile FWHM comparable to the electron transit times. Indeed, simulations using a time-dependent discrete dynode model[8] show that the gain of photoelectrons born 40 μm deep in the MCP can be higher than those born at the top for typical 0 or reverse bias camera operation at Nova. Hence, a transmission photocathode with enhanced quantum effiiciency at the top of the MCP would be desirable to reduce the fractional photoelectric contribution from the leaded glass.

2.2 Noise levels

The poor signal-to-noise characteristics of the MCP and film recording medium limit the minimum useful data bit size to well above the 27 μm FWHM MCP spatial resolution quoted above. For example, Nova 2D framing camera data which is near the saturation level, operated at all but the highest gain setting and digitized at 22 by 22 μm pixel size exhibits root-mean-square (RMS) intensity fluctuations on a flatfield image of ± 18% around the average exposure level (see Fig. 2). Independent measurements show 14% is due to the film (little difference between 2484 and TMAX 3200) and 12% is due to the combination of MCP pore-to-pore gain variations[16] and phosphor non-uniformities (little difference between aluminized[11] and the usual non-aluminized phosphors). By

comparison, input x-ray photon statistics are usually a negligible contributor of noise for most gain settings and usable signal levels on Nova framing cameras. Hence, for an acceptable RMS noise level of ≈ 5%, smoothing over a larger 66 by 66 μm size is necessary, dictating the large magnifications (e.g. 12X) used at Nova for ensuring 5 - 6 μm detector resolution at the object plane. Ring aperture coded imaging and applications where 1D averaging is possible may not be limited by signal-to-noise considerations and hence can make full use of the MCP resolution. However, for the more common 2D imaging usage, improvements in signal-to-noise should be possible since photon counting statistics have not been reached. For example, replacing the film recording medium with a low noise CCD could substantially reduce the 14% film noise level and the component of the 12% camera noise level that corresponds to the phosphor. Assuming pore-to-pore gain variations are independent of pore size for a given L/D plate, it is easy to show that by decreasing pore diameter, which is also recommended for increasing shutter speeds, the gain noise level will decrease proportionately.

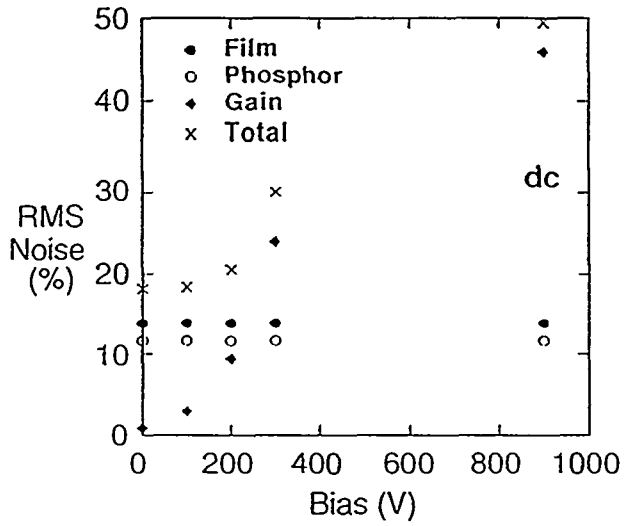

Figure 2 RMS noise contributions from film (solid circles), phosphor + MCP (open circles), photon statistics (diamonds) and quadrature total (crosses) as a function of bias voltage. For all bias voltages but 900 V, there is also a 200 ps FWHM 850 V peak pulsed voltage applied.

3. HARD X-RAY IMAGING

3.1 Current pinhole imaging

Pinhole arrays are the principle method of projecting multiple x-ray images on gated MCP detectors at Nova. Pinholes for 0.2- 7 keV x-ray imaging are laser-drilled in high-Z tantalum or tungsten substrates. The substrate thicknesses vary between 25 to 75 μm with maximum pinhole aspect ratios of ≈ 5 set by the laser drilling technique (e.g. 5 μm pinholes in 25 μm thick Ta). Typical camera magnifications M are 4 - 12X. We now consider the level of undesirable transmission of hard x-rays by these substrates.

Consider an idealized plasma emission source divided into two components: hard (≈ 10 keV) x-rays with intensity I_f transmitted through the pinhole substrate with optical depth t, and soft (few keV) x-rays with intensity I_s imaged by the 5 μm pinhole. Ignoring filters and spectral variations in detector sensitivity and assuming a

source size larger than the collimator diameter (e.g., 250 μm), the ratio of the hard x-ray exposure level O_f to the soft x-ray exposure level O_S is given by:

$$O_f/O_S = (250/5)^2(I_f\exp^{-\tau}/I_S) \quad (1)$$

Hence, hard and soft exposure levels will be comparable ($O_f = O_S$) when the ratio $I_f\exp\text{-}\tau/I_S$ reaches ≈ 0.04%. Figure 3 plots the transmission vs. photon energy through 25, 50 and 75 μms of Ta. For 25 μm Ta, the transmission ($\exp^{-\tau}$) rises above 1% just below the Ta L edge at ≈ 10 keV. Hence the ratio I_f/I_S in this case only needs to reach 4% for comparable 10 keV and soft x-ray exposures. Each additional 25 μm of Ta reduces the 10 keV x-ray transmission by a factor of ≈ 100. However, for > 30 keV emission, substantially more shielding is clearly needed. For example, > 200 keV photons from Nova laser plasma interactions have been observed by heavily shielded scintillators[17], attributed to bremsstrahlung emission from hot electrons slowing in the high Z Au hohlraum walls. The fogging situation is even worse than Eq. 1 suggests as the photoelectric response of the leaded MCP glass triples[13] between 5 and 20 keV, attributed to crossing the Pb L-edge and to an increase in the photoelectron range[18].

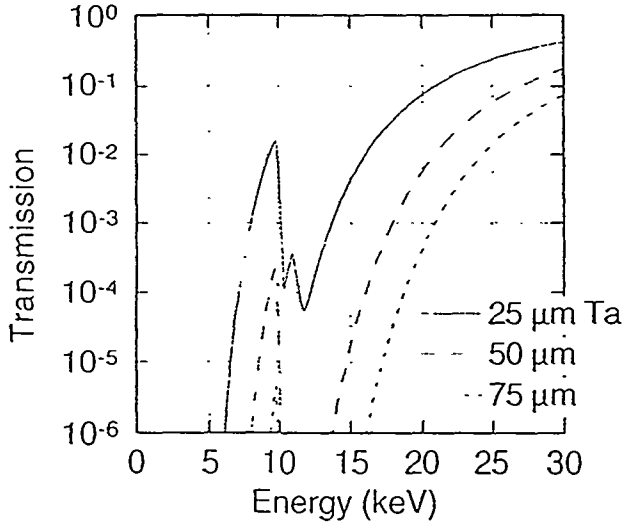

Figure 3 Transmission of 25, 50 and 75 μm Ta versus photon energy.

At Nova, hard (> 10 keV) x-ray fogging has been traditionally reduced by placing over the pinholes a second set of larger, 250 μm diameter holes drilled in 0.5 - 1 mm Ta. These "collimators" serve to limit the hard x-ray source size seen by any point on the detector to 250[(M+1)/M)] μm. Unfortunately, when imaging during the peak of a 30 TW laser-hohlraum interaction experiment, there is still insufficient rejection of hard x-rays leading to poor contrast (see Fig. 6). By reducing the collimator diameter from 250 to 75 μm, a 10x reduction in hard x-ray fogging should be realized according to Eq. 1. The difficulty with this arrangement is that precise microscope-based (< 30 μm tolerance) alignment of collimator holes and pinholes is needed, and the easily damaged pinhole substrate and small collimators must be glued together to ensure repeatable alignment, increasing fabrication costs. Clearly, different approaches to imaging will be needed. Moreover, for future ignition facility experiments, the expected large increases in target debris, opacity and in x-ray background due to increases in plasma temperature, volume and duration will require imaging at higher photon energies (5 - 15 keV), and will necessitate better schemes for mitigating ultra-hard x-ray fogging and instrument damage.

3.2 High aspect ratio pinhole imaging

Grazing incidence optics intrinsically provide hard x-ray rejection, but optics such as high-Z Kirkpatrick-Baez microscopes are currently limited[19] to < 8 keV imaging. Multilayer coated Wolter microscopes may be possible, relaxing the grazing incidence constraint, but unrealistic surface roughnesses approaching the atomic scale (Å) are still needed to avoid image blurring and scatter at 10 keV. Toroidally bent Bragg crystals show the most promise for reaching 10 keV, and have already demonstrated monochromatic imaging[20] of implosions at 3.5 keV. However, there are no immediate prospects for a true high (> 10 GHz) repetition rate framing camera, as is needed for implosion imaging, using only one optic. Hence, the optics fabrication costs and characterization efforts needed if say 16 optics were to replace 16 pinholes seem prohibitive. Therefore, we return to the idea of a simple pinhole optic and collimator array in a higher aspect ratio design. A fabrication technique for such pinholes comes from a Cornell group[7] which produced square 5 μm apertures with a 1000:1 aspect ratio. Briefly, 5 μm-deep grooves were first cut in two flat tungsten slabs. These slabs were clamped to two other flat slabs creating two 5 μm slits. The clamped slabs were then joined end-to-end but rotated 90° with respect to each other to create a 5 μm square pinhole from the projection of two crossed slits.

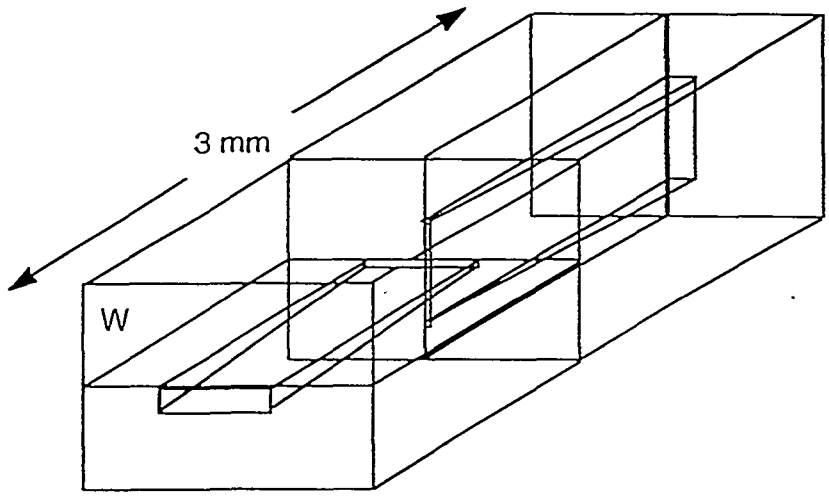

Figure 4 Schematic of one tapered pinhole fabricated from two crossed slits. The slits are shown as angled and tapered to accomodate a source that is down and left of the normal to the front surface of the substrate.

The technique has been extended to ICF diagnostics by creating 4 by 4 arrays of pinholes using a series of grooved, 1.5 mm-thick tungsten slabs sandwiched back-to-back and end-to-end (see Fig. 4). For an n by n array of n^2 pinholes, only 2(n + 1) pieces are needed. High aspect ratio slits for streaked imaging[21,22] and ring apertures for coded imaging[23] might also be easier to make this way. Clearly, tapered and angled grooves as shown in Fig. 4 are necessary to accomodate, respectively, finite source sizes and the multiple lines-of-sight normally inherent in ICF framing cameras. Given typical x-ray detector and source solid angles (< .003 steradian) and tilt tolerances (≤ .03 radians), taper opening angles need not exceed 100 mrad and can be customized for every line-of-sight by changing groove angle. An aspect ratio of 100 - 300 should then be feasible, a large improvement over the current aspect ratio of 10. For example, Fig 5 shows that unit optical depth is reached at 37 keV and again at 67 keV for the current 50 μm-thick Ta substrates while for a 0.5 (1.5) mm substrate, unit optical depth is only reached at 170 (260) keV. Note that the technique also offers a way of combining pinhole/slit, collimator and additional hard x-ray shielding into one robust piece which might survive longer and perhaps be cheaper in the long run. The modular design also allows for partial rather than total replacements of damaged parts and for multiple-size aperture usage

on a single shot. The only penalty might be a 25 - 50 μm uncertainty in the exact pinhole location, but this is unimportant in most cases, especially for implosion images and images containing spatial fiducials. High-aspect-ratio apertures might also make .1 - .3 MeV x-ray imaging an alternative to neutron imaging of fusion products.

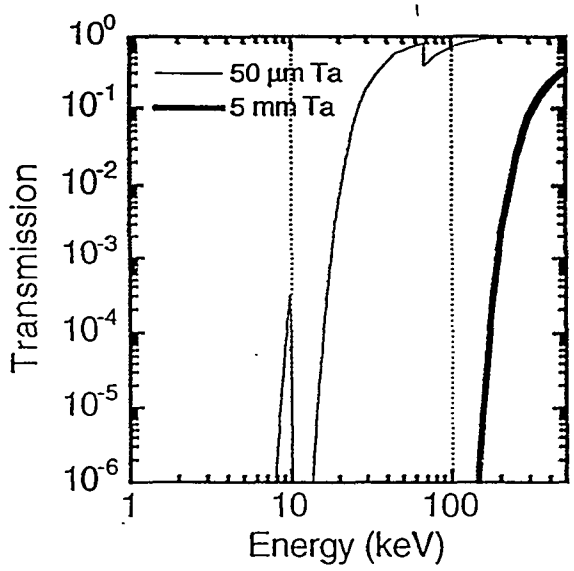

Figure 5 Transmission of 50 μm and 5 mm of Ta, showing effective extinction of < 200 keV radiation by mm-thick tapered pinhole design.

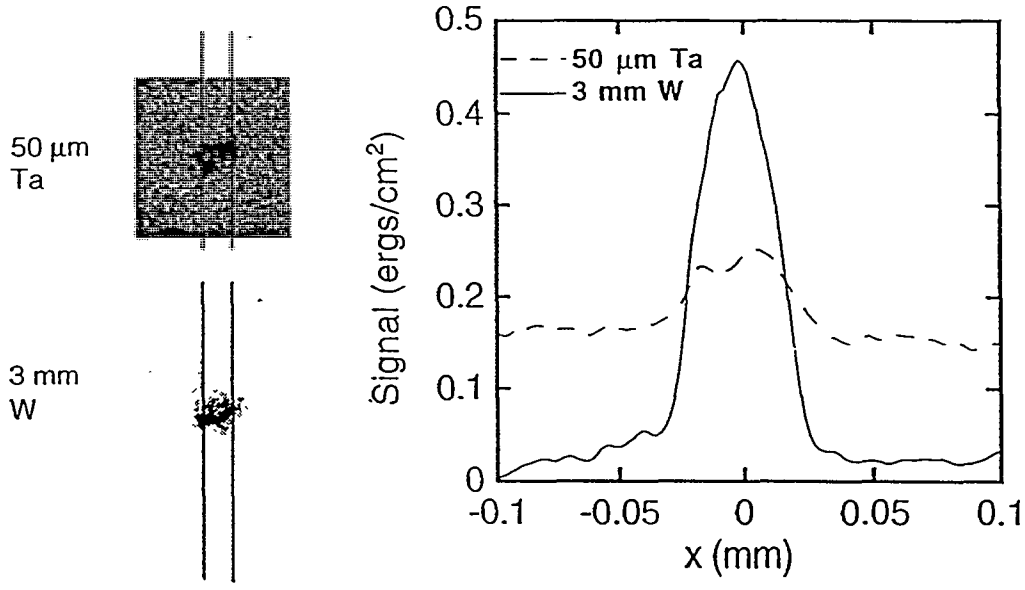

Figure 6 7 μm, 80 ps resolution, 6 keV images of compressed Ar-doped cores from x-ray driven capsules. Top image: Standard 25 μm-thick Ta substrate. Bottom image: High aspect ratio pinhole (3 mm W). Graph: Intensity lineouts for both showing 20x improvement in contrast for 3 mm W substrate.

Figure 6 shows 6 keV images of x-ray driven plastic capsule implosions[24] in hohlraums obtained at peak compression, at the end of a 2.2 ns-long laser pulse drive. The deuterium capsule fuel is doped with trace amounts of Ar to provide keV emission. Fig. 6 (top image) shows a typical image obtained by a 5 μm pinhole in standard 25 μm thick Ta while the bottom image was obtained by a 5 μm square pinhole, in a 3mm-thick, 12X version of the tapered pinholes. The taper cone angles were 3°, allowing for some tilt tolerance and providing a ≈ 1 mm field-of-view. The background diffuse emission which is strong for the standard substrate and practically non-existent for the 3 mm substrate represents Au plasma emission from 10^{15} W/cm^2 laser-plasma interactions in the mm sized hohlraum. Line-outs on the right show that a 20x improvement in contrast has been obtained by using the high aspect ratio pinhole. Similar or larger contrast enhancements have been recently obtained throughout the laser pulse duration using a 10μm, 8X version of the tapered pinhole for 4.7 keV backlit images of the imploding capsule. In this case, in order to accomodate a larger field-of-view (≈ 3 mm), the taper cone angles were set at 6°. With traditional.50 μm thick substrates, the hard x-ray fogging swamped these images rendering them unusable at the peak of the laser pulse.

4. SUMMARY

MCP-based x-ray framing cameras should still play a role in gated x-ray imaging at ICF facilities in the future. The trend towards imaging larger and higher temperature laser plasmas at higher photon energies (5 - 15 keV) will mean higher aspect ratio pinholes and thinner plates will be needed to mitigate hard x-ray fogging. Two prototype high aspect ratio pinholes deployed on Nova have greatly increased image contrast and clarity. The route of thinner, smaller pore single-plate designs also promises shorter gate widths. The problem of reduced gain due to the difficulty of driving lower impedance strip-lines on thinner plates should be compensated by direct CCD read-out of either the electrons exiting the MCP or the light from the phosphor conversion layer. In either case an improvement in signal-to-noise and hence effective spatial resolution is also anticipated, leading to reduced magnification requirements, relaxed alignment tolerances or larger fields-of-view. In addition, a high quantum efficiency front surface transmission photocathode will be desirable to reduce the importance of spatial and temporal blurring from the secondary volume photocathode represented by the leaded glass of the MCP.

5. ACKNOWLEDGMENTS

We thank L. Da Silva, J. Wiedwald, and B. Hammel for useful input and critique. This work was performed under the auspices of the U.S. Department of Energy by Lawrence Livermore National Laboratory under contract No. W-7405-ENG-48.

6. REFERENCES

1. M. Katayama, M. Nakai, T. Yamanaka, Y. Izawa and S. Nakai, "Multiframe x-ray imaging system for temporally and spatially resolved measurements of imploding inertial confinement fusion targets," Rev. Sci. Instrum. 62 (1991) 124.

2. D.K. Bradley, P.M. Bell, J.D. Kilkenny, R. Hanks, O. Landen, P.A. Jaanimagi, P.W. McKenty, and C.P. Verdon, "High-speed gated x-ray imaging for ICF target experiments," Rev. Sci. Instrum. 63 (1992) 4813.

3. P.M. Bell, J.D. Kilkenny, G. Power, R. Bonner, and D.K. Bradley, "Multiframe x-ray images from a single meander stripline coated on a microchannel plate," in Ultrahigh- and High Speed Photography, Photonics, and Videography '89, SPIE Vol. 1155 (SPIE, Bellingham WA, 1989), p. 430.

4. F. Ze, R.L. Kauffman, J.D. Kilkenny, J. Wiedwald, P.M. Bell, R. Hanks, J. Stewart, D. Dean, J. Bower, and R. Wallace, "A new multichannel soft x-ray framing camera for fusion experiments," Rev. Sci. Instrum. 63 (1992) 5124.

5. G.W. Fraser, M.A. Barstow, J.F. Pearson, M.J. Whiteley, and M. Lewis, "The soft x-ray detection efficiency of coated microchannel plates," Nucl. Instr. and Meth. 224 (1984) 272.

6. D.R. Marsh, O.H.W. Siegmund, and J. Stock, "Progress on high efficiency photocathodes for soft x-ray EUV and FUV photon detection," in EUV, X-ray, and Gamma-Ray Instrumentation for Astronomy IV, SPIE Vol. 2006 (SPIE, Bellingham WA, 1993), p. 51.

7. A.L. Ruoff, H. Luo, C. Vanderborgh, H. Xia, K. Brister, and V. Arnold, " Production and metrology of 5 μm x-ray apertures for 100 keV diffraction studies in the diamond anvil cell," Rev. Sci. Instrum. 64 (1993) 3462.

8. J.D. Kilkenny, "High speed proximity focused x-ray cameras," Lasers and Part. Beams 9 (1991) 49.

9. P.M. Bell, J.D. Kilkenny, O.L. Landen, D.K. Bradley, R.G. Watt, and J. Oertel, "Implementation of 40-ps high-speed gated-microchannelplate-based x-ray framing cameras on reentrant SIMs for Nova," in Ultrahigh- and High Speed Photography, Videography, and Photonics '94, SPIE Vol. 2273 (SPIE, Bellingham WA, 1994), p. 234.

10. D.K. Bradley, P.M. Bell, O.L. Landen, J.D. Kilkenny, and J. Oertel, "Development and characterization of a pair of 30 - 40 ps x-ray framing cameras," Rev. Sci. Instrum. 66 (1995) 716.

11. J.D. Wiedwald, P.M. Bell, J.D. Kilkenny, R. Bonner and D.S. Montgomery, "Recent advances in gated x-ray imaging at LLNL" in Ultrahigh- and High Speed Photography, Videography, and Photonics '90, SPIE Vol. 1346 (SPIE, Bellingham WA, 1990), p. 200.

12. S. Grantham, E. Miesak, P. Reese, and M. Richardson, "Optimum MCP configuration for use in high speed, high resolution x-ray imaging," in Ultrahigh- and High-Speed Photography, Videography, and Photonics '94, SPIE Vol. 2273 (SPIE, Bellingham WA, 1994), p. 108.

13. N. Yamaguchi, T. Cho, T. Kondoh, M. Hirata, S. Miyoshi, S. Aoki, H. Maezawa, M. Nomura, and Y. Satow, "Characterization of microchannel plates for plasma x-ray diagnostics in the 0.6 - 82 keV energy range," Rev. Sci. Instrum. 60 (1989) 2307.

14. O.L. Landen, P.M. Bell, J.A. Oertel, J.J. Satariano, and D.K. Bradley, "Gain uniformity, linearity, saturation and depletion in gated microchannel-plate x-ray framing cameras" in Ultrahigh- and High-Speed Photography, Videography, and Photonics '93, SPIE Vol. 2002 (SPIE, Bellingham WA, 1993), p. 2.

15. O.L. Landen, A. Abare, B.A. Hammel, P.M. Bell, and D.K. Bradley, "Detailed measurements and shaping of gate profiles for microchannel-plate-based x-ray framing cameras," in Ultrahigh- and High Speed Photography, Videography, and Photonics '94, SPIE Vol. 2273 (SPIE, Bellingham WA, 1994), p. 245.

16. R.L. Bell, "Noise figure of the MCP image intensifier tube," IEEE Trans. on Electron Devices," ED-22 (1975) 821.

17. R.A. Lerche, D.W. Phillion, and G.L. Tietbohl, "25 ps neutron detector for measuring ICF-target burn history," Rev. Sci. Instrum. 66 (1995) 933.

18. J.E. Bateman, "The detection of hard x-rays (10-140 keV) by channel plate electron multipliers," Nucl. Instr. and Meth. 144 (1977) 537.

19. F.J. Marshall and Q. Su, "Quantitative measurements with x-ray microscopes in laser-fusion experiments," Rev. Sci. Instrum. 66 (1995) 725.

20. I. Uschmann, E. Forster, H. Nishimura, K. Fujita, Y. Kato, and S. Nakai, "Temperature mapping of compressed fusion pellets obtained by monochromatic imaging," Rev. Sci. Instrum. 66 (1995) 734.

21. B.A. Remington, B.A. Hammel, O.L. Landen, and R.A. Pasha, "High energy x-ray imaging diagnostic on Nova," Rev. Sci. Instrum. 63 (1992) 5083.

22. B.A. Hammel, D. Griswold, O.L. Landen, T.S. Perry, B.A. Remington, P.L. Miller, T.A. Peyser, and J.D. Kilkenny,"X-ray radiographic measurements of radiation-driven shock and interface motion in solid density material," Phys. Fluids B5 (1993) 2259.

23. D. Ress, R.A. Lerche, and L. Da Silva,"Demonstration of an x-ray ring-aperture microscope for inertial confinement fusion experiments," Appl. Phys. Lett. 60 (1992) 410.

24. O.L. Landen, C.J. Keane, B.A. Hammel, M.D. Cable, J. Colvin, R. Cook, T.R. Dittrich, S.W. Haan, S.P. Hatchett, R.G. Hay, J.D. Kilkenny, R.A. Lerche, W.K. Levedahl, R. McEachern, T.J. Murphy, M.B. Nelson, L. Suter and R.J. Wallace, "Indirectly Driven, High Growth Rayleigh-Taylor Implosions on Nova," to be published in Jour. Quant. Spectr. and Radiat. Trans. (1995).